SLAC-PUB-1482
September 1974
(T)

THEORIES OF HIGH TRANSVERSE MOMENTA PHENOMENA*

J. F. Gunion

University of Pittsburgh, Pittsburgh, Pennsylvania 15213,

Max Planck Institut fur Physik, Munich, Germany

and

Stanford Linear Accelerator Center
Stanford University, Stanford, California 94305

Presented at the 17th International Conference on High Energy Physics, Imperial College, London, England, 1-10 July 1974.

*Supported in part by the National Science Foundation and in part by the U.S. Atomic Energy Commission.

The development of the quark parton model as an explanation of the scaling observed in deep inelastic electron nucleon and (less directly) neutrino nucleon scattering is now ancient history. However, the only additional leptonic test, that of scaling in e^+e^- annihilation, has proven, viewed optimistically, inconclusive. Surprisingly the principle support for naive composite theories of the hadron has come from the arena of hadron physics--scattering processes at large transverse momenta. Within the constituent interchange model[1-3] (CIM) a fairly tight framework is capable of unifying and describing a large body of experimental facts. This framework is based upon two principle ingredients

a) the quark model of hadrons

$$p = qqq + (q\bar{q} \text{ pairs})$$
$$\pi = q\bar{q} + (q\bar{q} \text{ pairs})$$

b) an interaction between quarks characterized by a dimensionless coupling constant, or constants, which for fermion quarks implies a vector gluon theory.

One then makes two assumptions[4] which imply the absence of anomalous dimensions on the quark level at high p_T:

i) quark wave functions within hadrons are finite at the origin;

ii) the kernel describing the interaction between quarks has the same asymptotic properties as a simple gluon exchange.

The asymptotic properties of high p_T processes involving hadrons are then easily obtained. Because of i), the kernel, K, is exposed the minimal number of times required in order that the quarks "directly emitted" by the hadrons be in the low transverse momentum region of the hadronic wave function. A large angle or high p_T process is then averaged over probable configurations. This is illustrated, for the case of the pion form factor, in Fig. 1.

Assumption ii) then tells us that the quark amplitude has at high p_T naive, dimensionally, determined asymptotic behavior. For example from Fig. 1, $F_\pi(t) \sim \frac{1}{t}$. In general if a given state, i, of a hadron consists of N_i quarks, the contribution to the hadron form factor behaves as

$$F(t) \overset{t \to \infty}{\sim} \frac{1}{t^{N_i - 1}} \tag{1}$$

(Thus the valence state of the proton yields dipole behavior.) According to the Drell-Yan-West (DYW) relation[5], this then implies that the probability distribution function, $f(x)/x$, for a quark in state i of the hadron behaves as[6,7,8]

$$f(x) \overset{x \to 1}{\sim} (1 - x)^{2N_i - 3} \tag{2}$$

(x represents the fraction of hadron momentum carried by the quark.) It should be noted that the DYW relation can be proven[6] given b), i) and ii) provided one demands that Z graphs involving bound state constituents be suppressed. Such suppression (not yet shown to hold in any theory) is required in order that hadronic amplitudes not have $J = 0$ fixed poles.[9] Equation (2) can be tested indirectly by examining the existing deep inelastic data.[6] The 1st nonvalence nucleon state consists of 5 quarks, for which $f(x) \propto (1 - x)^7$. By associating this threshold damping with the Regge and Pomeron (or "sea") components of quark distribution functions and by employing sum rules, it is possible to extract[6] very satisfactory qqq, valence state, distributions, another "success" of this approach. Finally we may also use (2) to obtain the probability distributions of hadrons within hadrons.[6,8] A nonvalence state quark may be viewed as arising from the valence state of a secondary hadron which in turn originated from the primary hadron, Fig. 2. Formally

$$f_{\bar{q}/H}(x) = \int_x^1 f_{H'/H}(z)\, f_{\bar{q}/H'}(x/z)\, dz \tag{3}$$

This hadronic bremsstrahlung formula requires, for consistency, that

$$f_{H'/H}(z) \overset{z \to 1}{\sim} (1 - z)^{2N_{\bar{H}'H} - 1} \tag{4}$$

$N_{\bar{H}'H}$ is the minimum possible number of quarks in an $\bar{H}'H$ state. Thus for instance, if $H = p$, $H' = \pi$, $q = \bar{\lambda}$, we obtain $f_{\pi/p} \overset{z \to 1}{\sim} (1 - z)^5$ from Eq. (4) which solves (3) ($7 = 5 + 1 + 1$; one of the 1's arises from the integration limits). These results for $f_{H'/H}(z)$ and $f_{q/H}(x)$ will be particularly important in high p_T inclusive predictions. It also seems that the behaviors suggested for $f_{H'/H}$ may be directly observable in the "usual" triple Regge region (at small t).[8,6] The effective trajectories extracted from the data strongly suggest the presence of hadronic bremsstrahlung processes.[8] Let us now turn to exclusive scattering.

The fixed angle, $s \to \infty$, behavior of exclusive hadronic scattering amplitudes is easily obtained, using the techniques sketched earlier for form factors. We find[4,10]

$$s^2 \frac{d\sigma}{dt} \overset{\text{Fixed Angle}}{\sim} A^2 \sim \left(\sqrt{s}^{\,4-n_A-n_B-n_C-n_D}\right)^2 \Theta_{ABCD}(z_{CM}) \qquad (5)$$

where hadron A contains n_A quarks, etc. (z_{CM} is the center of mass scattering angle.) Two types of contributing diagrams are illustrated for the case of πp scattering in Fig. 3(a,b). Each yields, in agreement with (1),

$$\frac{d\sigma}{dt} \sim \frac{1}{s^8}\, \Theta(z_{CM}) \qquad (6)$$

However, the experimentally observed angular distribution is most consistent with the CIM diagram of Fig. 3a; the "Chou Yang" diagram of Fig. 3b must be considerably suppressed at fixed angles. This is difficult to justify, but a number of possibilities suggest themselves:

i) The intermediating kernel, K_{CY}, is a colored octet member while hadrons are color singlets; (two vector gluon exchange would also be numerically suppressed because $8 \times 8 \Longrightarrow$ many things in addition to a singlet);

ii) K_{CY} is suppressed relative to the other kernels because of the off shell quark configuration;

iii) the diagram of Fig. 3b is not, of itself, suppressed, but after s channel iteration (or eikonalization) it is, at fixed angle. This possibility seems appealing as the (quantum number singlet portion of the) net result might then be identified with the diffractive contribution to elastic scattering.[11]

The situation is further complicated by the fact that, in general, the "multiple scattering" diagram type of Fig. 3c must be included (illustrated for $\pi\pi$ scattering). Here the quarks are not forced off shell but phase space suppresses the amplitude at fixed angle, $s \to \infty$, yielding cross sections of the general form (6) but with weaker s fall off. Again experiment is not consistent with such an energy dependence. These diagrams were discussed by Landshoff[12] and possible reasons for their absence (which fall under (ii), above) were considered by Polkinghorne.[12]

In any case the angular dependences predicted at large angle by CIM diagrams are, generally, remarkably good for meson-baryon reactions. The $K^{\pm}p$ reactions are dramatic examples (Fig. 4).

Proton proton elastic scattering is more troublesome.[13] The predicted power dependence

$$\frac{d\sigma}{dt} \sim \frac{1}{s^{10}} \, \Theta(z_{CM}) \qquad (7)$$

while not bad, is not good either. The naive expectations for $\Theta(z_{CM})$ are also imperfect. Inclusion of quark pairing effects[14] or logarithmic power modifications (such as those associated with asymptotically free theories) may be required to fit the data.

We now come to the most dramatic evidence in favor of the picture suggested so far--high p_T inclusive reactions.[15-18] Again there are two principle parton model process types, illustrated in Fig. 5. (We do not attempt to discuss the many other mechanisms proposed.[19-21]) The first, the "Chou Yang" process,[22] proceeds via emission of a quark from each of the two incoming particles. These then scatter to produce quarks at high p_T, one of which turns into the observed hadron. At 90°_{CM}, for instance, the prediction is that $E(d\sigma/d^3p) \sim 1/p_\perp^4 F'(x_\perp = 2p_\perp/\sqrt{s})$, essentially because the controlling subprocess of qq scattering is characterized by $d\sigma/dt \sim 1/s^2$ by Eq. (5). (Note that $d\sigma/dt$ and $E(d\sigma/d^3p)$ have the same dimensions.) F' can be predicted, but the $1/p_\perp^4$ behavior is inconsistent with current data. Perhaps K_{CY} is again suppressed by one of the mechanisms considered earlier. (Case i) requires further assumptions concerning the communication between high p_T jets, and case ii) becomes more difficult as well.)

The second process illustrated, Fig. 5b, is one of several CIM processes.[2,23,8] The asymptotic behavior of the one drawn is controlled by quark pion scattering at fixed angle, $(d\sigma/dt)^{q\pi \to q\pi} \sim 1/s^4$ by Eq. (5), so that

$$E\frac{d\sigma}{d^3p} \overset{90^\circ_{CM}}{\sim} \frac{1}{p_\perp^8} F(x_\perp) \tag{8}$$

$F(x_\perp)$ is completely determined by the counting rules given earlier. We have

$$\frac{1}{p_\perp^8} F(x_\perp) = \int f_{\pi/p}(z)\, dz \int f_{q/p}(x)\, dx \; \left.\frac{d\sigma}{dt}\right)^{q\pi \to q\pi}_{xzs,zt,xu} s\delta(xzs + zt + xu) \tag{9}$$

with $t = u = p_\perp\sqrt{s}$ at 90° in the center of mass; (tu symmetrization is necessary away from 90°). $f_{\pi/p} \sim (1 - z)^5$ and $f_{q/p} \sim (1 - x)^3$. The δ function, which assures that the $q\pi \to q\pi$ fixed angle, subprocess (evaluated at reduced energy and momentum transfer) is on shell, restricts the x and z integrals so that

$$F(x_\perp) \sim (1 - x_\perp)^{9=5+3+1} \tag{10a}$$

Other parton CIM diagrams yield

$$F(x_\perp) \sim (1 - x_\perp)^{11} \tag{10b}$$

The prediction, Eqs. (8) and (10), is in remarkable agreement with the ISR π^0 data at 90°. In order to compare to lower energy N.A.L. data it is necessary to consider also $1/p_\perp^{12}$ terms. These arise from diagrams such as that of Fig. 6. (Note that to the extent such a diagram contributes overall baryon quantum numbers should characterize the particles opposite the observed π.) The "kernel" subprocess $q(q \text{ pair}) \to \pi + B^*$ has $d\sigma/dt \sim 1/s^6$ at fixed angle; also $f_{q/p} \sim (1 - x)^3$, $f_{q\ \text{pair}/p} \sim (1-x)$ so that

$$E \frac{d\sigma}{d^3p} \overset{90^\circ}{\sim} \frac{1}{p_\perp^{12}} (1 - x_\perp)^{5=3+1+1} \tag{11}$$

Thus, in general, we must write

$$E \frac{d\sigma}{d^3p} \overset{90^\circ}{\sim} \frac{F(x_\perp)}{p_\perp^8} + \frac{1}{p_\perp^8} \frac{G(x_\perp)}{s^2} \tag{12}$$

F and G may be extracted from the NAL data at any given $x_\perp$ using various pairs of the three available energies, 200, 300 and 400 GeV.

The results are given in Fig. 7, along with sample theoretical curves, for a number of interesting cases. The inconsistency of the data with Eq. (12), measured by the error bars in the figures, is in general small and within experimental errors. (The consistency level is not so high for $F(x_\perp)$ for p and $\bar{p}$ observation. This will be discussed elsewhere.) It should, in any case, be noted that features, such as the more rapid fall off of $G^{\bar{p}}$, compared to G^{p}, with $x_\perp$ are natural consequences, in this approach, of the difference in the quark constituency of the observed particles; all such $x_\perp$ behaviors are well determined by the counting rules already given.[8,23]

Let us now elaborate on some of the exclusive and inclusive predictions of this approach. Concerning the former, it should be stressed that interchange theory provides a uniform link between the backward and forward Regge regions.[13] The only other type of theory, capable of doing so, is one characterized by logarithmic trajectories.[13] In fact the CIM angular dependences can be rephrased in terms of predictions for the large t (or u) limits of Regge trajectories.[24,25,4]

The general rule takes the form

$$\alpha_{\mathrm{eff}}^{A\bar{B}}(t) \xrightarrow{s \gg t_{AB} \gg m^2} \frac{1}{2}(4 - n_A - n_B - n) + n_{SF} \tag{13}$$

where n is the minimum number of quarks that can be exchanged in the $A\bar{B}$ channel of a CIM dual-like diagram. n_{SF} is a helicity flip correction necessary when spin considerations are incorporated.

$$\alpha_{\mathrm{eff}}^{\mathrm{pp\ elastic}}(t) \longrightarrow -2 \qquad \text{(forward)}$$

$$\alpha_{\mathrm{eff}}^{\mathrm{p\bar{p}\ elastic}}(u) \longrightarrow -4 \qquad \text{(backward)}$$

$$\alpha_{\mathrm{eff}}^{\pi\pi\ \mathrm{elastic}}(t) \longrightarrow -1 \qquad \text{(forward)}$$

$$\alpha_{\mathrm{eff}}^{\pi p \to \pi p}(u) \longrightarrow -3/2 \qquad \text{(backward)} \qquad n_{SF} = 1/2$$

The behavior of the Regge residues is then immediate from Eqs. (13) and (5). It is interesting to note[25] that these results along with standard factorization for Regge trajectories require that in pp elastic scattering the various higher lying πp and $\pi\pi$ trajectories (which couple, as one moves towards the forward direction, to pp elastic) must in fact cancel at fixed angle. This will obviously make pp phenomenology somewhat tricky.

Particularly interesting special cases are those corresponding to exotic trajectories. For instance for $\pi p \to \varphi n$ one predicts in the forward direction $\alpha_{\mathrm{eff}}^{\pi-\varphi\ \mathrm{channel}}(t) \to -3$; i.e., $d\sigma/dt)_{t\,\sim\,0}$ should fall as $1/s^8$ if the interchange graph prediction is relevant.

In inclusive scattering a number of particularly interesting results also emerge.[1,2,8,23] Especially important are the photon induced reactions such as $\gamma p \to \pi^+ + X$. One finds a number of possible contributions which roughly take the form

$$E \frac{d\sigma^{\gamma p \to \pi}}{d^3p} \underset{\sim}{90^\circ} \begin{cases} \dfrac{(1-x_\perp)^3}{p_\perp^6} \quad \text{and} \quad \dfrac{(1-x_\perp)^3}{p_\perp^8} \\ \\ \dfrac{(1-x_\perp)^0}{p_\perp^{12}} \quad \text{and} \quad \dfrac{(1-x_\perp)^1}{p_\perp^{12}} \\ \\ \begin{array}{c}\text{point like photon}\\ \text{component}\end{array} \quad \begin{array}{c}\text{vector meson dominated}\\ \text{component}\end{array} \end{cases} \tag{14}$$

The upper contributions will clearly dominate for $x_\perp$ not near 1 provided $p_\perp$ is large enough. The bottom two always win for $x_\perp \to 1$ the phase space limit and, in fact, appear to provide a nice description of existing low energy data. Also of great importance are meson beam experiments.[26] For instance $\pi^+ p \to \pi^+ + X$ should have the originally discussed direct scattering term which for $x_\perp \to 1$ (at 90°) is damped only minimially

$$E \frac{d\sigma^{\pi^+ p \to \pi^+ + X}}{d^3p} \underset{\sim}{90^\circ} \frac{1}{p_\perp^8} (1 - x_\perp)^3 \tag{15}$$

whereas for $\pi^+ p \to \pi^- + X$ such a minimally damped term should be absent. In addition direct measurement of this term will be a great help in determining the normalization of the "kernel" $q\pi \to q\pi$ amplitude which controls $p_\perp^8$ scaling in $pp \to \pi + X$.

It should also be stressed that Eq. (9) is easily evaluated away from 90° in the C.M. One finds that in the central region, i.e., t and u of order $p_\perp \sqrt{s}$, and in the high p_T triple "Regge" region, the typical cross section takes the form

$$E \frac{d\sigma}{d^3p} \overset{A+C \to C+X}{\sim} \begin{cases} \epsilon^P/(p_\perp^2)^N & \text{Central} \\ \epsilon^{\alpha(0)-2\alpha_{A\bar{C}}(t)}\,\beta(t) & \text{"Triple Regge"} \end{cases}$$

where $\epsilon = 1 - \sqrt{x_T^2 + x_L^2}$, the ratio of missing mass^2 to s, approaches 0 near the kinematical limit. (x_L is the usual Feynman longitudinal momentum fraction of the observed particle.) The triple Regge $\alpha_{A\bar{C}}(t)$ is exactly that expected in the CIM for the exclusive limit process (where ϵ is of the order of $1/s$). $\beta(t)$ is, of course, predicted. The power P controlling the central region as $\epsilon \to 0$ is completely determined, for any given graph, by the type of counting rules already discussed.

Finally we will turn to a number of topics of current interest. First is the question of the multiplicity distribution opposite the observed high $p_\perp$ particle.[27] In a process such as that of Fig. 5b the final quark (which is presumed to turn into the observed hadrons) is not generally opposite the observed pion. The CM of the $q\pi$ "kernel" amplitude is not necessarily the same as the proton proton CM.

The quark distribution as a function of rapidity, η, is easily obtained, for instance, for the two configurations measured by one of collaboration at ISR.[28] For a π^0 at 90° a plateau of width ~ 2.5 in rapidity (at $p_\perp \approx 3$) is predicted for the quark distribution. Of course, the quark must turn into hadrons but the experimental rapidity width may be a bit wide to be fully reproduced. If one measures a high p_T π^0 away from 90° (say at $\eta = +.5$) the quark distribution is generally peaked in the opposite rapidity direction (equal negative rapidity) in agreement with experiment. It should be noted that for some types of interactions (i.e. "kernel" processes) quite different results can be obtained. For instance, for the same two situations, the diagram of Fig. 5a yields a very broad distribution (η width > 4) at 90°. Sufficiently unusual "kernel" processes or sufficiently high p_T (away from the phase space boundary) can even result in a peak shift, for the opposing multiplicity, in the same direction in η as that at which the π^0 is observed.

The final topic I wish to discuss is the relation of the naive predictions, presented thus far, to more sophisticated models of the hadronic interactions--in particular asymptotically free theories and "bag" models. As mentioned earlier, the fixed angle behavior of, for instance, pp elastic scattering will be modified in an asymptotically free theory. These modifications may be explored using an intuitive approach in which the effective number of constituents increases, as the momentum transfer with which the hadronic wave function is being probed increases, due to (massless) vector gluon straggling.[29] For asymptotically free theories this increase in number goes like $\ell n\, \ell n(t)$ (t is the momentum transfer). This type of approach is relevant to calculating the modifications expected to graphs of the interchange type using the counting rules already given. (We ignore Landshoff's type of graph, for instance.) One obtains a result of the form (for pp elastic)

$$\frac{d\sigma}{dt}\overset{90°}{\sim} \frac{1}{(s/2)^{10 + a\, \ell n[\ell n(s/2)/\ell n\, u_0]}} \sim \frac{1}{s^{n_{eff}}} \qquad (16)$$

For favorite SU(3) color theoretical parameters $a = 32/27$ and the choice $u_0 = 10$ is made in order to obtain a reasonable description of the slightly faster then dipole fall off of the proton form factor. (We also have set the usual scale parameter to 1 GeV^2.) One finds

$$n_{eff} \sim 10.5 \qquad s/2 \sim 10 \sim 20 \ \mathrm{GeV}^2$$

$$\sim 11.5 \qquad s/2 \sim 20 \sim 30 \ \mathrm{GeV}^2$$

This yields a nice fit to the 90° pp data. A closely related description[30] of the pp elastic data is that using the Baker Coon logarithmic trajectoried dual model[31] for which $n_{eff} \sim a + b \ \ell n \ s/2$. This behavior corresponds to a "fixed point" gauge theory in which the Callan Symanzik β function forces the coupling constant to some finite value at large momenta.

The above results seem quite encouraging. However the modifications, using the same scale factors and colored gluon model parameters to $p_\perp^8$ scaling at ISR then turn out to be massive, Fig. 8. The principal source of breakdown is that the $q\pi$ "kernel" interchange amplitude no longer behaves as (roughly) $1/(\alpha p_\perp^2)^4$ but rather as

$$\frac{1}{(\alpha p_\perp^2)^{4 + a \ \ell n[\ell n(\alpha p_\perp^2)/\ell n \ u_0]}} .$$

α is determined by the convolution integral of Eq. (9) and is such that α is ≈ 2. Then $\alpha p_\perp^2$ at $x_\perp = .25$ varies from $\approx$ 25 GeV^2 to 75 GeV^2 as $\sqrt{s}$ varies from 30 to 50. The situation is further worsened by the fact $q\pi \to q\pi$ amplitude acts as an effective current on the $f_{\pi/p}$ and $f_{q/p}$

distribution functions which in asymptotically free theories receive both multiplicative logarithmic damping modifications and logarithmic modifications to the $(1 - x)$ and $(1 - z)$ powers controlling $f_{\pi/p}$ and $f_{q/p}$. The effective Q^2 of this current, $z\, p_\perp \sqrt{s}$ in Fig. 5b, varies, on the average, from 40 to 120 GeV^2. Of course fixed point theories are much worse, still. The possibility that the field theory diagrams neglected in the CIM approach might restore $p_\perp^8$ scaling cannot be ruled out but certainly the CIM approximation would have to break down.

It would seem, though that the bag model,[32] in which the quark gluon coupling can be made arbitrarily small without destroying the hadronic state spectrum could be capable of explaining naive $p_\perp^8$ scaling at ISR energies. The kernel $K, (\xi)$, is then more complicated to interpret as it represents the interaction of a quark with the walls of the collective bag state. The normalization of this interaction need have no relation to the gluon coupling constant.

REFERENCES

1. J. F. Gunion, S. J. Brodsky, and R. Blankenbecler, Phys. Rev. D6, 2652 (1972); Phys. Letters 42B, 461 (1972).
2. J. F. Gunion, S.J. Brodsky, and R. Blankenbecler, Phys. Letters 39B, 649 (1972); Phys. Rev. D8, 287 (1973).
3. P.V. Landshoff and J.C. Polkinghorne, DAMTP preprints 72/43; 72/48; 73/16 (1972, 1973); Phys. Letters 45B, 361 (1973); Phys. Rev. D8, 927 (1973) criticize and extend the approach of Refs. 1 and 2.
4. S. J. Brodsky and G. R. Farrar, Phys. Rev. Letters 31, 1153 (1973); V. Matveev, R. Muradyan,and A. Tavkhelidze, Nuovo Cimento Letters 7, 719 (1973). See also Z. F. Ezawa, DAMTP 74/15.
5. S. D. Drell, T. M. Yan, Phys. Rev. Lett. 24, 181 (1970); G. West, Phys. Rev. Letters 24, 1206 (1970).
6. J. F. Gunion, "Isolating the 3-quark component ..." PITT-120 (1973), Phys. Rev. to be published.
7. G. R. Farrar, CALT-63-422, January 1974.
8. S. J. Brodsky, R. Blankenbecler, SLAC PUB - 1430, May 1974.
9. These $J = 0$ fixed pole ideas were developed with S. J. Brodsky.
10. These results are all the same as those originally obtained in Ref. 1 except for baryon-baryon elastic scattering, where quark pairing was assumed in Ref. 1.
11. The approaches of L. Durand and R. Lipes, Phys. Rev. Letters 20, 637 (1968) and R. Suaya and C. Dominguez, SLAC-PUB are not unrelated to this possibility.

12. P. V. Landshoff, DAMTP 73/36; J. C. Polkinghorne, Phys. Letters 49B, 277 (1974).

13. J. Tran Than Van, J. F. Gunion, D. Coon and R. Blankenbecler, SLAC-PUB.

14. J. F. Gunion, PITT-116 "Quark pairing..." see also Ref. 6.

15. F. W. Busser et al. Phys. Letters 44B, 471 (1973).

16. M. Banner et al., Phys. Letters 44B, 537 (1973).

17. B. Alper et al., Phys. Letters 44B, 521 (1973).

18. V.W. Cronin et al., Phys. Rev. Letters 31, 1426 (1973).

19. D. Cline, F. Halzen and H. Waldrop, Nuclear Phys. B55, 157 (1973). M. Bander, R. M. Barnett, and D. S. Silverman, Phys. Letters 48B, 1974

20. G. Preparata, CERN preprint TH 1859 (1974).

21. D. Amati, L. Caneschi, and M. Testa, Phys. Letters 43B, 186 (1973).

22. S. M. Berman, J. D. Bjorken, and J. Kogut, Phys. Rev. D4, 3388 (1971); J. D. Bjorken, Phys. Rev. D8, 4098 (1973); S. D. Ellis and M. B. Kislinger, Phys. Rev. D9, 2027 (1974).

23. J. F. Gunion, S. J. Brodsky, and R. Blankenbecler, PITT preprint.

24. This approach was emphasized in J. F. Gunion, Pavia Conference Proceedings, 1973 as well as in Refs. 13 and 8.

A related discussion is given by V. Matveev, R. Muradyan and A. Tavkkelidze in a paper submitted to the London (1974) Conference.

25. M. Blankenbecler, S. J. Brodsky, J. F. Gunion and R. Savit, SLAC-PUB-1294.

26. This is of course the original process of Ref. 2. The importance of direct measurements has been reemphasized by B. Combridge DAMTP preprint.

27. J. F. Gunion, in preparation, S. D. Ellis, CERN, has also computed such distributions.

28. B. Betev et al., paper (1038), London Conference.

29. J. Kogut and L. Susskind, Cornell preprint (1973) emphasize this approach to gauge theories. D. Gross and S. Treiman, Phys. Rev. Letters 32, 1145 (1974) and A. de'Rujula, Phys. Rev. Letters, ibid. p. 1143 do as precise a job as one can, for the colored quark model, in applying asymptotic freedom to form factor behavior.

30. J. Tran Than Van, D. Coon and V. Sukhatme, Phys. Letters B45, 287 (1973).

M. Arik PITT-119 to be published.

31. M. Baker and D. Coon, in preparation.

32. A. Chodos et al., MIT preprint.

Figure Captions

1. Form factor of a pion in a "vector gluon" theory.

2. Consistency requirement for the hadronic bremsstrahlung picture of antiquark distributions in a proton.

3. a) Interchange Diagram Topology for $MB \to MB$.

   b) "Chou Yang" topology for $MB \to MB$

   c) Landshoff or "multiple scattering" topology for $MM \to MM$.

4. K^+p and K^-p elastic scattering angular distributions.

5. a) Chou Yang and b) Sample Interchange diagram for inclusive production of pions at large transverse momentum.

6. A second type of interchange diagram for high p_T pion production with $1/p_T^{12}$ behavior.

7. a) $F(x_\perp)$ for $x_\perp > .3$ for π^+ and π^- production in proton Tungsten collisions.

   b) $G(x_\perp)$ for $x_\perp > .3$ for π^+ and π^- production.

   c) $G(x_\perp)$ for $x_\perp > .3$ for p and $\bar{p}$ production.

   Sample theoretical predictions for each are given. Error bars indicate inconsistency level (i.e. degree to which more terms than $1/p_\perp^8$ and $1/p_\perp^{12}$ are required).

8. Illustration of $p_\perp^8$ scaling breakdown when asymptotically free gauge theory corrections are incorporated in the CIM diagrams.

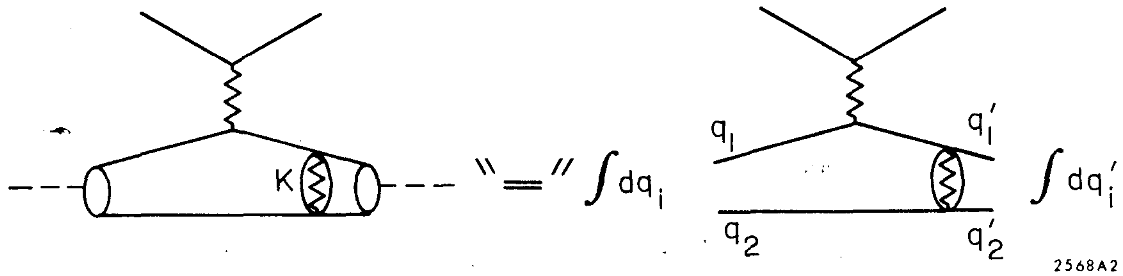

Fig. 1

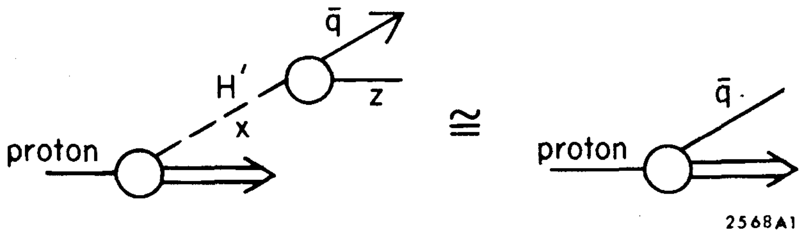

Fig. 2

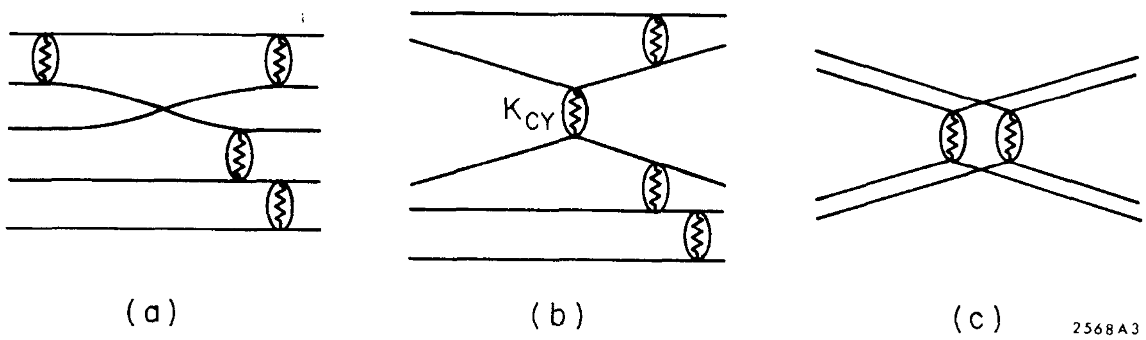

Fig. 3

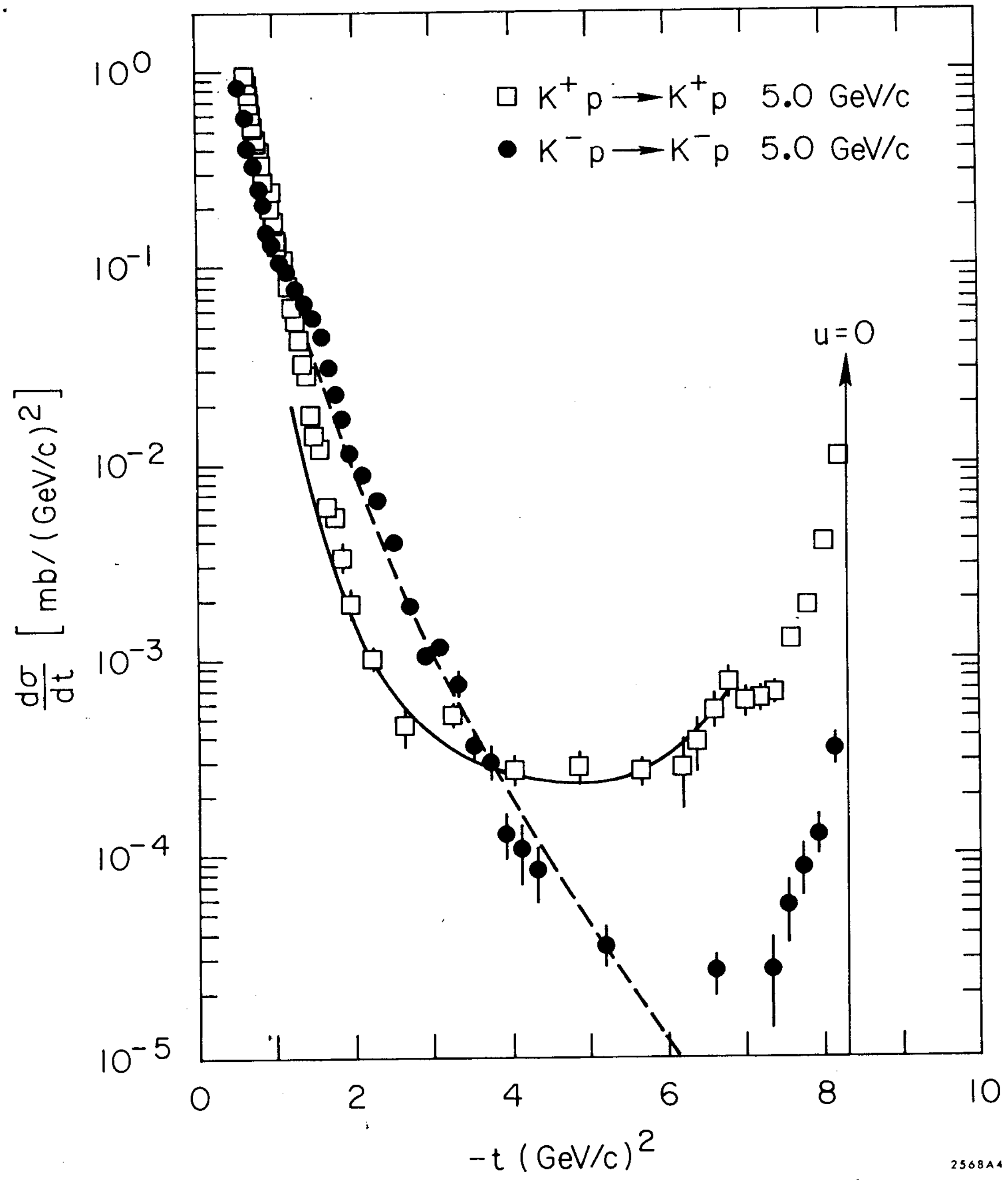

□ K⁺p → K⁺p 5.0 GeV/c
● K⁻p → K⁻p 5.0 GeV/c
u=0
$\frac{d\sigma}{dt}$ [mb/(GeV/c)^2]
10^0
10^{-1}
10^{-2}
10^{-3}
10^{-4}
10^{-5}
0
2
4
6
8
10
$-t$ (GeV/c)^2
2568A4

Fig. 4

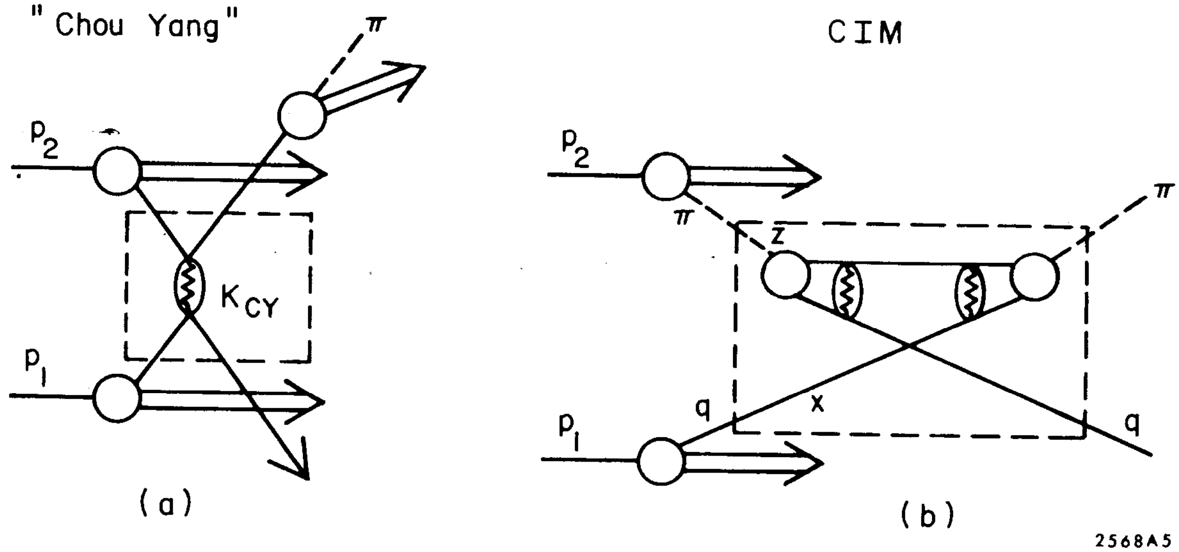
"Chou Yang"
π
p_2
K_{CY}
p_1
(a)
CIM
p_2
π
π
z
q
x
q
p_1
(b)
2568A5

Fig. 5

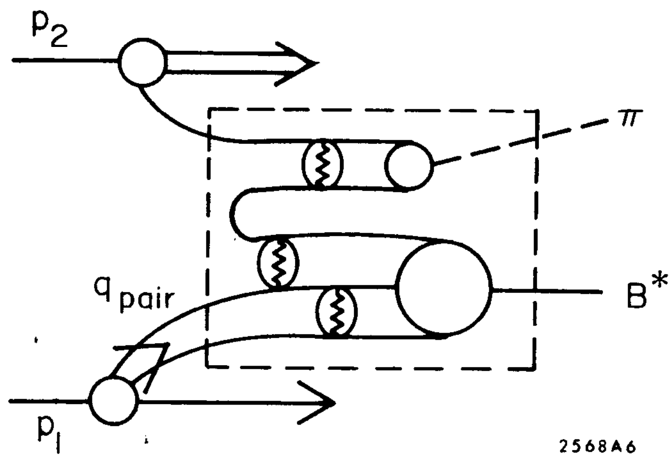
p_2
π
q_{pair}
B^*
p_1
2568A6

Fig. 6

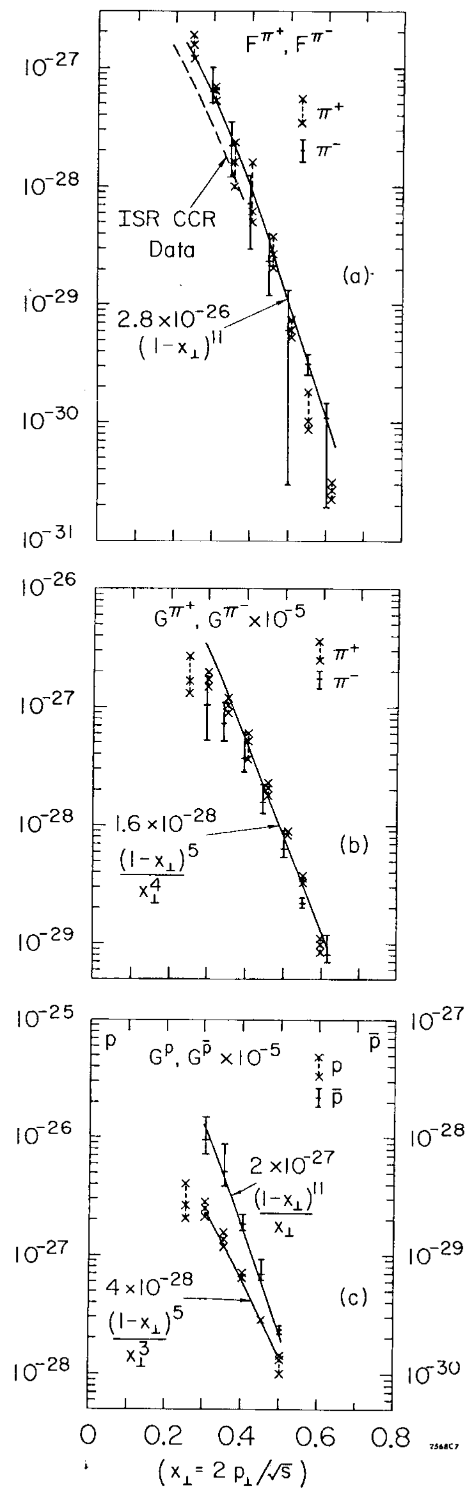

10^{-27}
10^{-28}
10^{-29}
10^{-30}
10^{-31}
F^{π^+}, F^{π^-}
π^+
π^-
ISR CCR Data
(a)
2.8×10^{-26}
$(1-x_\perp)^{11}$
10^{-26}
10^{-27}
10^{-28}
10^{-29}
$G^{\pi^+}, G^{\pi^-} \times 10^{-5}$
π^+
π^-
1.6×10^{-28}
$\frac{(1-x_\perp)^5}{x_\perp^4}$
(b)
10^{-25}
10^{-26}
10^{-27}
10^{-28}
10^{-27}
10^{-28}
10^{-29}
10^{-30}
p
$\bar{p}$
$G^p, G^{\bar{p}} \times 10^{-5}$
p
$\bar{p}$
2×10^{-27}
$\frac{(1-x_\perp)^{11}}{x_\perp}$
4×10^{-28}
$\frac{(1-x_\perp)^5}{x_\perp^3}$
(c)
0
0.2
0.4
0.6
0.8
$(x_\perp = 2p_\perp/\sqrt{s})$

Fig 7

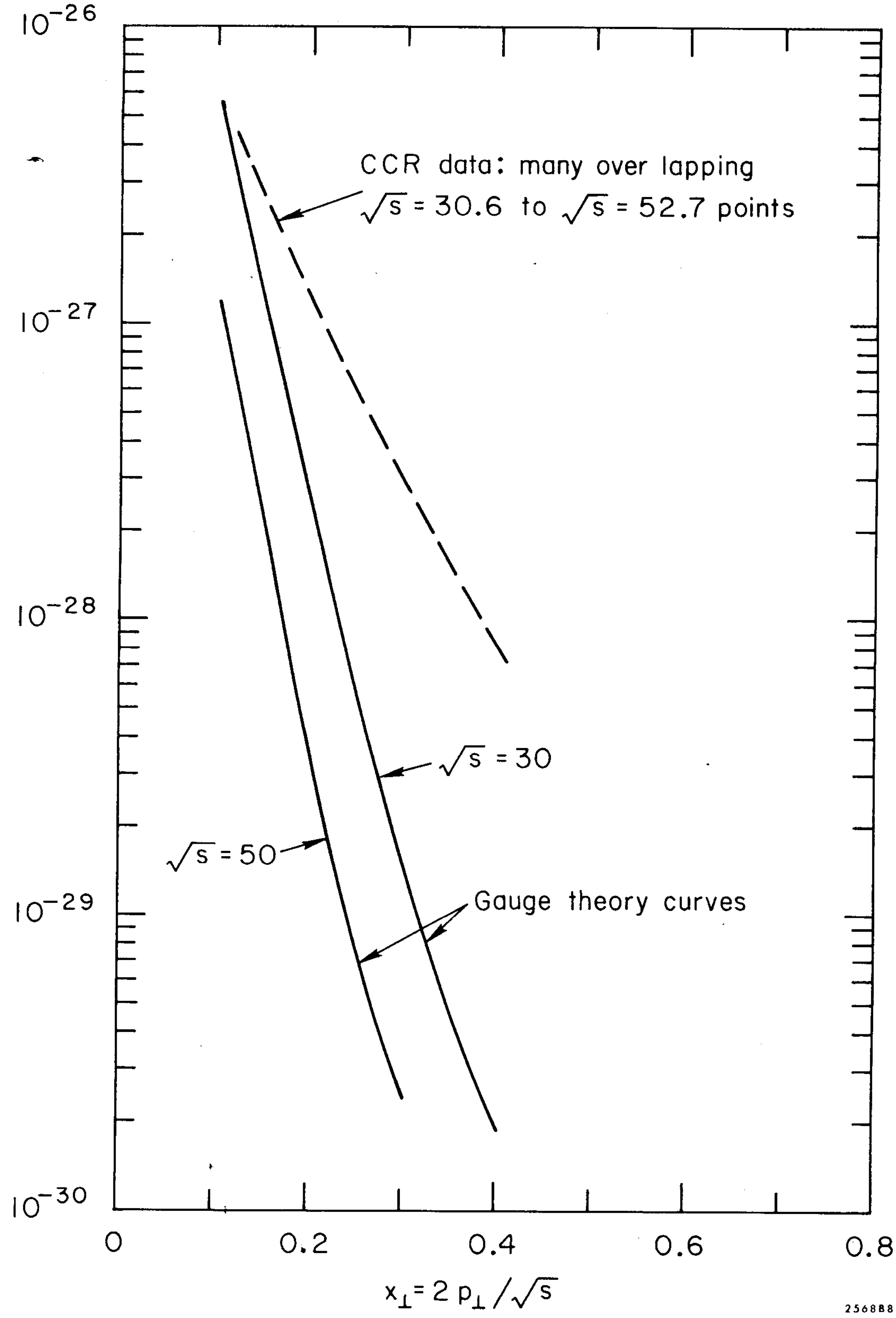

10^{-26}
10^{-27}
10^{-28}
10^{-29}
10^{-30}
$p_\perp^8 \; E \frac{d\sigma}{d^3p}$
CCR data: many over lapping
$\sqrt{s}$ = 30.6 to $\sqrt{s}$ = 52.7 points
$\sqrt{s}$ = 30
$\sqrt{s}$ = 50
Gauge theory curves
0
0.2
0.4
0.6
0.8
$x_\perp = 2\, p_\perp / \sqrt{s}$
256888

Fig. 8

February 1975

RE: SLAC-PUB-1482, "Theories of High Transverse Momenta Phenomena," by J. F. Gunion

Figure 8 in PUB-1482 is incorrect. The proper Figure 8 is printed on this sheet. Please replace this in your copy of the PUB.

SLAC Technical Information Dept.